Iraqi National Journal of Earth Sciences, Vol. 21, No. 2, pp. 63-77, 2021

Reservoir Characterization of the Middle Cretaceous Mishrif Formation in the Buzurgan Oilfield, Southern Iraq

Muneef M. Mohammed
Dept. of Petroleum and Refining Engineering College of Petroleum and Mining Engineering, University of Mosul

Hameed M. Salih
North Oil Company Ministry of Oil

Kadhim H. Mnaty
Missan Oil Company Ministry of Oil

(Received 25/9/2021 , Accepted 25/12/2021)

ABSTRACT

The Mishrif Formation is considered the main oil reservoir in the Buzurgan oilfield, southern Iraq. This study aims to characterize and evaluate the reservoir properties of the Mishrif Formation based on the interpretation of well logs data. The logs data for six wells have been analyzed and interpreted by using Techlog 2015.3 software. The lithology of the Mishrif Formation was determined by using the M-N cross plot method based on the interpretation of density, neutron, and sonic logs. The results showed that the Mishrif Formation is mainly composed of limestone. The shale volume in the Mishrif Formation has been estimated from the gamma-ray log. The results illustrated that the shale volume is about 20% of the bulk volume, and may increase to reach the highest value at the upper part of the MA unit of the formation. The porosity of the Mishrif Formation was calculated based on the interpretation of neutron, density, and sonic logs. To achieve accurate values of porosity, the log-derived porosity has been correlated with the core-derived porosity, and the comparison showed a good correlation between the two types of porosity. The results showed that the Mishrif Formation is characterized by low to medium porosity (about 5% to 18%). The secondary porosity of the formation is most dominant in the MB21 unit compared with the other stratigraphic units of the Mishrif Formations. This indicates that the MB21 unit was affected by the diagenesis processes. The MB21 unit of the Mishrif Formation represents the most dominant reservoir because it was delineated by high effective porosity and high oil saturation.

Keywords: Mishrif Formation; Buzurgan oil field; Effective porosity; Water saturation

التوصيف المكمني لتكوين المشرف (الكريتاسي الأوسط) في حقل البزركان النفطي، جنوب العراق

منيف محجوب محمد
قسم هندسة النفط والتكرير
هندسة النفط والتعدين- جامعة الموصل

حميد محمود صالح
شركة نفط الشمال
وزارة النفط

كاظم حمود مناتي
شركة نفط ميسان كلية
وزارة النفط

الملخص

يعتبر تكوين المشرف أحد المكامن النفطية المهمة في حقل البزركان النفطي في جنوب العراق. تهدف هذه الدراسة الى توصيف وتقييم الخصائص المكمنية لتكوين المشرف اعتمادا على تفسير سجلات الابار. تم تحليل بيانات السجلات لستة ابار وتفسيرها باستخدام برنامج Techlog. تم تحديد اللثولوجي لتكوين المشرف اعتمادا على تفسير مجسات الكثافة، النيوترون والمجس الصوتي. أظهرت النتائج ان تكوين المشرف يتكون بشكل أساسي من الحجر الجيري. تم تقدير حجم السجيل في تكوين المشرف من تفسير مجس اشعة كاما، حيث أوضحت النتائج ان حجم السجيل يبلغ حوالي 20% من الحجم الكلي. تم حساب مسامية تكوين المشرف بناءا على تفسير مجسات النيوترون، الكثافة والمجس الصوتي. ولغرض الحصول على قيم دقيقة للمسامية، تم مضاهاة قيم المسامية المشتقة من تسجيلات الابار مع القيم المشتقة من تحليل اللباب الصخري، حيث أظهرت المضاهاة وجود تطابق جيد بين القيم. أظهرت النتائج بان تكوين المشرف يتصف بقيم مسامية واطئة الى متوسطة (حوالي 5% الى 18%)، وأن المسامية الثانوية هي المسامية السائدة في الوحدة الطباقية (MB21) مقارنة مع الوحدات الطباقية الأخرى للتكوين. بينت الدراسة أن الوحدة الطباقية (MB21) لتكوين المشرف تمثل المكمن الابرز بسبب كونها تمتاز بقيم عالية للمسامية الفعالة ودرجة تشبع النفط.

الكلمات الدالة: تكوين مشرف، حقل بزركان النفطيو المسامية الفعالة، التشبع المائي.

INTRODUCTION

The Mishrif Formation is considered one of the main oil carbonate reservoirs in the Mesopotamian Basin, and it contains about 30% of the proven oil reserves in Iraq (Al-Sakini, 1992). The formation was firstly described in southern Iraq by Owen and Nasr (1958). The Mishrif formation is described by an organic detrital limestone with algal, rudist, and coral-reef limestones (Bellen, *et al.*, 1959). In the type area, the formation is composed of dense, algal limestones with gastropods shell fragments above, and of detrital, porous, and foraminiferal limestones with rudist debris below (Jassim and Goff, 2006). The formation was deposited in a carbonate platform ramp environment (Al-Ali, *et al.*, 2019), and it is composed of bioclastic-detrital limestone with rudist, algal, and coral facies (Al-Ameri et al., 2009). Four facies have been recognized in the Mishrif Formation, and these facies are restricted shelf, rudist build-up, open shelf, and sub-basinal (Sherwani and Mohammed, 1993; Aqrawi et al., 1998). The rudist build-up is the main reservoir rock in the Mishrif Formation, and this facies has been divided into three sub-facies based on the relative content of micrite and the coarseness of the rudist-derived material (Alkersan, 1975; Aqrawi *et al.*, 1998). The rudist facies of the Mishrif Formation is considered the best hydrocarbons reservoirs in southern Mesopotamian due to the presence of interconnected vugs in grain-dominated fabric (Mahdi, *et al.*, 2013). The Mishrif Formation was divided into seven stratigraphic units (MA, MB11, MB12, MB21, MB22, MC1, and MC2) (Reulet, 1970). The MB21 unit is considered the main oil-bearing reservoir in the Buzurgan oil field, and the main lithology of this unit is composed of bioclastic limestone (rudist and grainstone) and chalky limestone (Sang, *et al.*, 2017). The Mishrif Formation has been divided into two main reservoirs in the Nasiriya oilfield (Al-Khafaji, 2015). In Halfaya oilfield, various types of grain shoal reservoirs that are dominated by grainstone and wackestone packstone characterize the formation (Jun, *et al.*, 2016).

The main aim of the study is to characterize and evaluate the reservoir characteristics of the Mishrif Formation, which represents the main hydrocarbon reservoir in the Buzurgan oilfield. The study involves lithological analysis and determination of reservoir characteristics of the formation such as porosity and oil saturation based on the interpretation of logging data.

LOCATION AND GEOLOGICAL SETTING

The Buzurgan oilfield is located about 40 km to the northeast of Amara City, the south-eastern part of Iraq (Al-Ameri, *et al*., 2015) (Fig. 1). The field has been discovered in 1970, and the development stage of the field was started in 1976. Tectonically, the Buzurgan oilfield forms part of the unstable platform – Mesopotamian Basin zone (Buday, 1980). The structure of the field represents an asymmetrical anticline that extends at NW-SE direction with 40km length and 7km width and has two domes (north and south) which are separated by a saddle (Aldarraji and Almayahi, 2019) (Fig. 2).

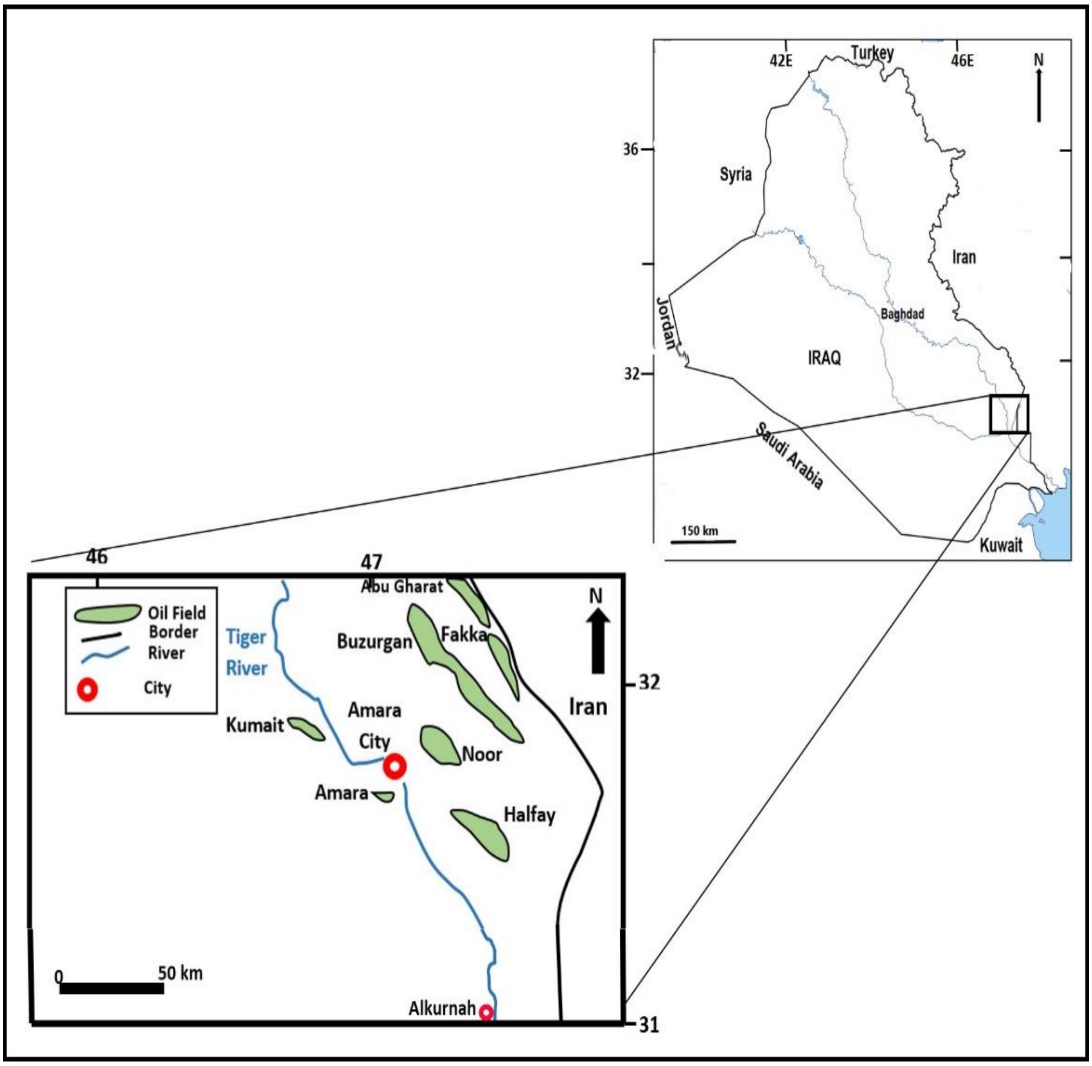

Fig.1: The map of Iraq showing the location of the Buzurgan oilfield (modified from Al-Ameri, *et al*., 2015).

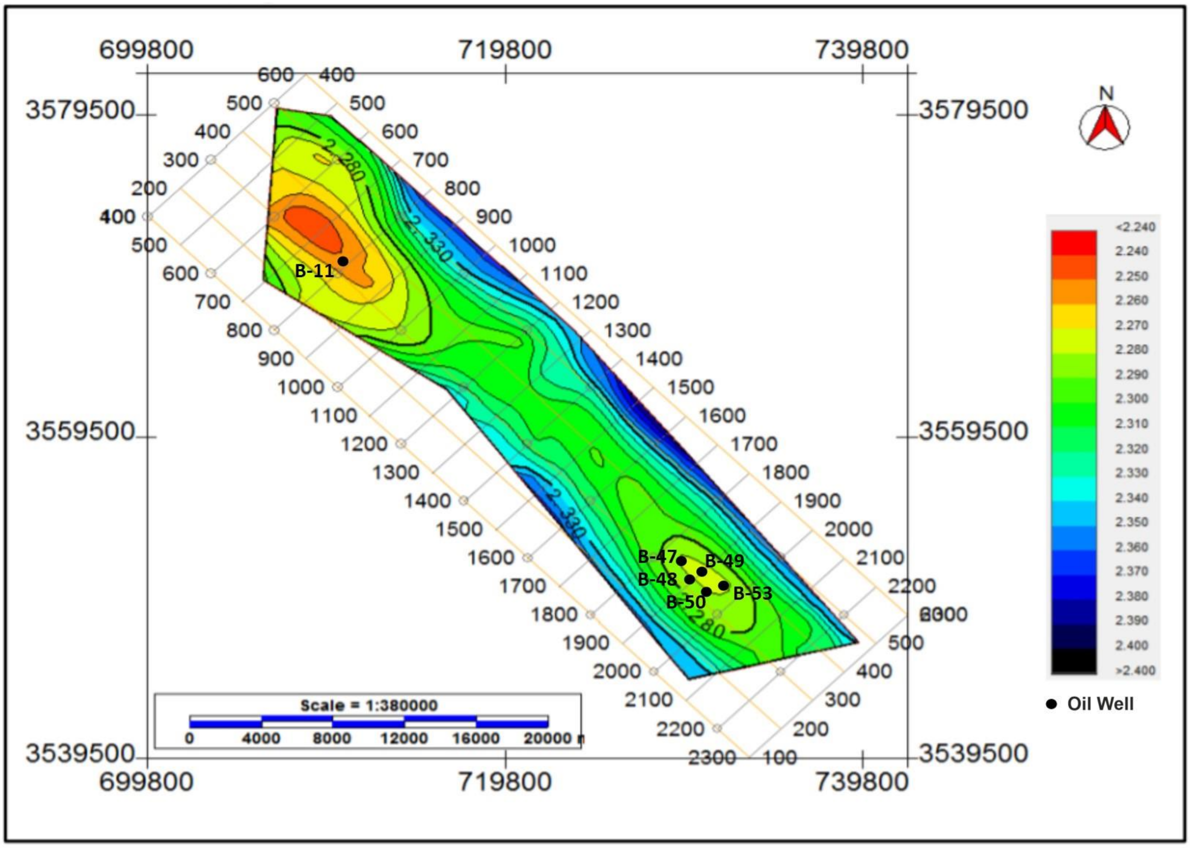

Fig. 2: Time structural map of the top of the Mishrif Formation in the Buzurgan oilfield showing the location of studied wells (modified from Aldarraji and Almayahi, 2019).

MATERIALS AND METHODS

The study was built on using the logs data of six wells of Buzurgan oilfield to determine the lithology and reservoir properties of the Mishrif Formation. Five of these wells (B-47, B-48, B-49, B-50, and B-53) are located in the southern dome of the Buzurgan structure, whereas the sixth well (B-11) is located in the northern dome (Fig. 2). The raw data of the available open hole logs (Self Potential, Gamma Ray, Resistivity, Density, Sonic, and Neutron) of these wells were used in this study. The Microsoft Excel, Didger, and Schlumberger Techlog software were used in preparing, digitizing, analysis and interpretation the logs.

The methodology that was used in this study has been divided into three main stages. Firstly, the logs data for the six wells have been digitized and converted from graphical data into digital data by using Didger software and Microsoft Excel software. Secondly, the digital logs data were loaded into the Schlumberger Techlog 2015.3 software for interpretation. Finally, the log data have been analyzed and interpreted by using Schlumberger Techlog 2015.3 software to determine the lithology and reservoir properties of the Mishrif Formation. The lithology of the Mishrif Formation was determined by using the M-N cross plot method, which is based on the use of density, neutron, and sonic logs. The M and N were calculated as shown in the following two equations (Schlumberger, 2011):

$$\mathbf{M} = \frac{\Delta t_f - \Delta t}{\rho_b - \rho_f} \times \mathbf{0.01} \qquad (1)$$

$$N = \phi_{NF} \text{-} \phi_N / \rho_b \text{-} \rho_f \qquad (2)$$

Where: M is the Lithology indicator, N is the Lithology indicator, Δt_f= Transit Time of the Fluid in the formation in µsec/ft, Δt is the Transit Time in the formation (from the log in µsec/ft), ρ_b is the Formation Bulk Density (from density log in gm/cc), ρ_f is the fluid density in gm/cc, ϕ_N is the Neutron derived porosity (%), and ϕ_{NF} = 1.

The shale volume in the Mishrif Formation was determined based on the interpretation of the gamma-ray log. Firstly, the gamma-ray index (I_{GR}) was estimated according to the equation (Schlumberger,1972):

$$\mathbf{I_{GR} = (GR_{log} - GR_{min}) / (GR_{max} - GR_{min})} \quad (3)$$

Where: $\mathbf{I}_{GR}$ is the index of gamma-ray, $\mathbf{GR}_{log}$ is the reading of gamma-ray log in the studied zone (3700 – 425 m.) (API units), $\mathbf{GR}_{min}$ is the minimum reading of gamma-ray log in a shale-free zone (API units), $\mathbf{GR}_{max}$ is the maximum reading of the gamma-ray log in the shale zone (API units).

The second step was the calculation of the shale volume (Vsh) of the Mishrif Formation by using the Larionov' equation that is used for older than Tertiary age successions (Larionov,1969):

$$\mathbf{V_{sh} = 0.33 * \left[2^{(2*IGR)} - 1\right]} \quad (4)$$

Where: $\mathbf{V_{sh}}$ is the shale volume (decimal fraction), $\mathbf{I}_{GR}$ is the gamma-ray index (from equation 3).

The porosity of the Mishrif Formation was calculated based on the interpretation of different logs and using many equations. The total porosity was calculated based on the neutron and density logs and by using the following equation (Schlumberger,1974):

$$\mathbf{\phi_{ND} = (\phi_N + \phi_D) / 2} \quad (5)$$

Where: $\boldsymbol{\phi}_{ND}$ is the porosity that was calculated from neutron and density logs (combination neutron-density log) (%), $\boldsymbol{\phi}_N$ is the porosity that was derived from neutron log (%), $\boldsymbol{\phi}_D$ is the porosity that was derived from the density log (%).

The secondary porosity was calculated by the secondary porosity index (SPI) (Schlumberger,1989):

$$\mathbf{SPI = \phi_{ND} - \phi_s} \quad (6)$$

Where: SPI is the index of secondary porosity (%), $\boldsymbol{\phi}_{ND}$ is the total porosity (%) and $\boldsymbol{\phi}_s$ is the sonic (primary porosity) (%).

Effective porosity has been calculated by using the following equation that represents the relationship between total and effective porosities (Schlumberger,1972):

$$\mathbf{\phi_{eff} = \phi_{ND} * (1 - V_{sh})} \quad (7)$$

Where: $\boldsymbol{\phi}_{eff}$ is the effective porosity (decimal fraction), $\boldsymbol{\phi}_{ND}$ is the total porosity (decimal fraction) and $\mathbf{V}_{sh}$ is the shale volume (decimal fraction). To achieve accurate values of porosity, the log-derived porosity values have been correlated with the core-measured porosity values that were calculated from the core analysis for two wells (BU-1 and BU-11). The values of core-measured porosity were plotted against the log-derived porosity (log effective porosity) on a linear-linear scale to define the relationship between the two measured porosities.

The water saturation of the formation was calculated by using Archie's equation, which reflects the relationship between the resistivity and porosity as:

$$\mathbf{Sw} = \left(\frac{\mathbf{a*Rw}}{\mathbf{Rt*Ø^m}}\right)^{\mathbf{1/n}} \qquad (8)$$

Where: S_w is the water saturation (decimal fraction), R_w is the resistivity of formation water (0.0165 ohms.m), R_t is the true formation resistivity (ohm.m), Ø is the porosity, a is the tortuosity (a=1), n is the saturation exponent (n= 2) and m is the cementation factor (m= 2).

The formation water resistivity (R_w) value has been collected from Missan Oil Company, whereas the true resistivity value was estimated from the resistivity log. The values of a, n, and m parameters have been calculated by using the Pickett plot method, which involves plotting the true resistivity values against the porosity values on a logarithmic scale (Pickett, 1973).

RESULTS AND DISCUSSION

1. Recognition of lithology:

The lithology type of the Mishrif Formation has been recognized by using the M-N cross plot method. In all studied wells, the M-N cross plot data are concentrated on the calcite area (Fig. 3). This indicates that the Mishrif Formation is fundamentally consisting of limestone. The result coincides with the previous studies which pointed out that the Mishrif Formation is mainly consisting of limestone (for example Aqrawi, *et al*., 1998; Mahdi, *et al*., 2013).

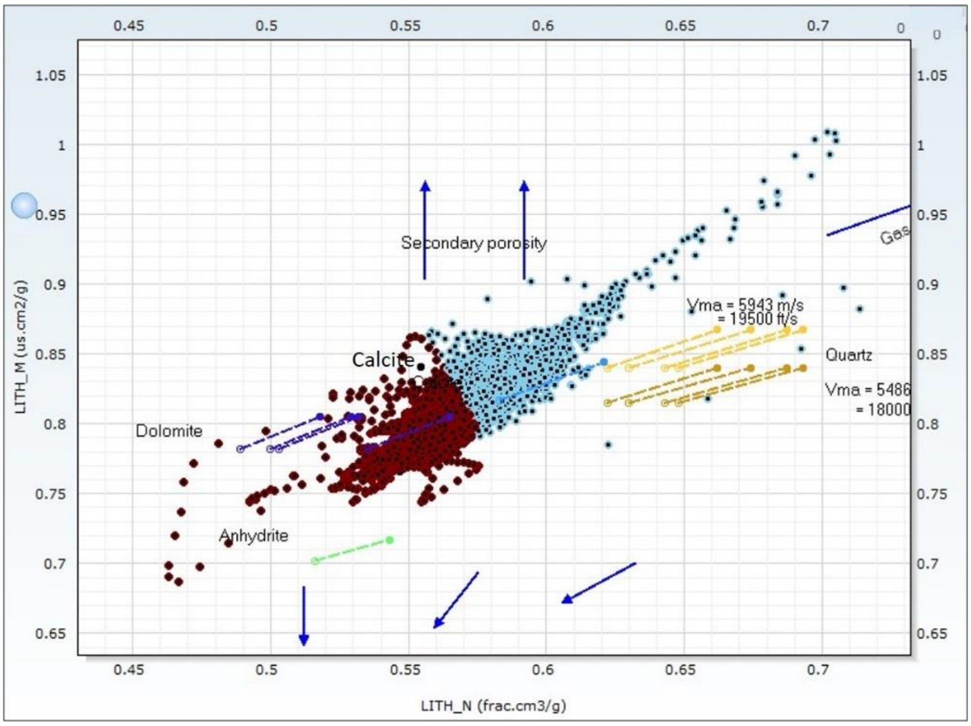

Fig. 3: The M-N cross plot of the well B-50, which was derived from the interpretation of the density, neutron, and sonic logs. The blue points represent high porosity whereas the red points represent low porosity.

2. Calculation of shale volume:

The shale content has an impact on the reservoir's properties such as porosity and water saturation, therefore it must be considered when dealing with the petrophysical evaluation of the hydrocarbon reservoirs (Bassiouni, 1994). Figure 4A shows the shale volume in B-11 and B-47 wells. The results showed that the shale volume in the Mishrif Formation generally ranges from 15% to 22% of the bulk volume, and may increase to reach the highest value at the top of the MA unit (Fig. 4A) and (Table 1).

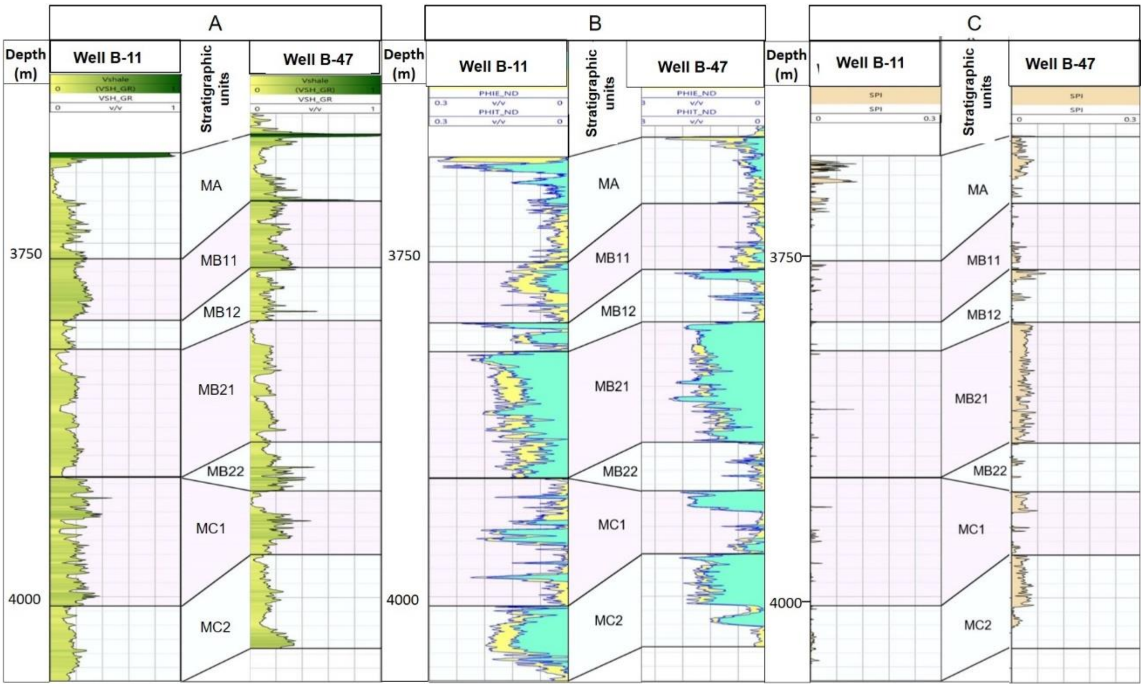

Fig. 4: Comparison of the petrophysical properties of the Mishrif Formation between well B-11 and well B-47. (A) shale volume, (B) effective and total porosities, where effective porosity is shown in greenish-blue as a continuous log plotted above the total porosity, which is shown in yellow, (C) secondary porosity index.

Table 1: Shows the average values of the shale volume (Vsh) of the stratigraphic units of the Mishrif Formation.

Stratigaphic units	Average V_{sh} (%)
MA	20
Mb11	22
Mb12	18
Mb21	15
Mb22	20
Mc1	22
Mc2	18

3. Calculation of porosity:

Porosity is a fundamental property of reservoir rocks that determines the potential storage capacity of fluids (e.g. oil, water) (Schon, 2011). The total porosity of the Mishrif Formation was estimated based on the interpretation of neutron and density logs. The results showed that the total porosity or neutron-density porosity of the Mishrif Formation ranges between (5% to 18%), and the MB21 unit of the formation has the maximum value (about 18%) as shown in Fig. 4C.

The secondary porosity is defined as the type of porosity that developed after the deposition of sediment because of the geological processes (diagenesis and tectonic) (Tiab and Donaldson, 2012). This type of porosity is more developed in carbonate rocks than in siliciclastics, and this is can be related to the effect of the diagenesis processes on the carbonate rocks. The secondary porosity index (SPI) of the Mishrif Formation was estimated based on the difference between total porosity and primary porosity. The primary porosity of the Mishrif Formation was calculated from the sonic log record. The results showed that the secondary porosity of the Mishrif Formation is generally ranging between (2% – 5%) (Fig. 4B). Also, Fig. 4B showed that the secondary porosity has been well developed at the MB21 unit of the formation.

The effective porosity is considered more important than total porosity because it represents the percentage of interconnected pore spaces that are used in the estimation of recoverable hydrocarbon reserves. Figure 4C illustrates the relationship between the effective porosity and total porosity of the Mishrif Formation in the Buzurgan oil field as derived from well log analysis. The results showed that the effective porosity has been well developed in the MB21 unit (about 14%) compared with the other units of the Mishrif Formation.

The measurements of core-porosity are considered as an accurate source for getting formation porosity. The core measurements throughout the formation interval are un-continuous due to the very high cost of coring operation. Therefore, the integration of the well logs and core porosity values is required to calibrate the calculated porosities by logs. In this study, the core-derived porosity data in well B-11 have been collected from Missan Oil Company. The available core-derived porosity values are limited at depths ranging from 3800 m. to 3960 m. within the MB12, MB21, and MC1 units.

To achieve accurate porosity values of the Mishrif Formation, the neutron-density (total) porosity values were firstly compared with the available core-derived porosity values for MB12, MB21, and MC1 units (Fig. 5). The results showed the neutron-density porosity matching the trend of core-derived porosity but shows a bit lower values than the core-derived porosity (Fig. 5). The log-derived porosity values were correlated and integrated with the core-derived porosity values, and the results showed a good correlation between the porosity values (Fig. 6). This correlation has been used to predict and estimate the porosity values of the other stratigraphic units.

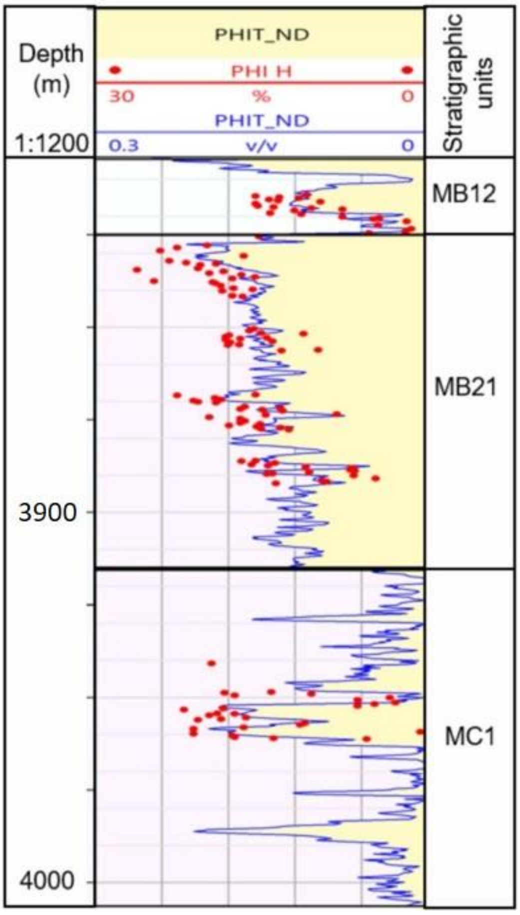

Fig. 5: Neutron-density derived porosity compared with core-derived porosity of B-11 well. The red dots represent the laboratory core porosity and the continuous log represents the total porosity.

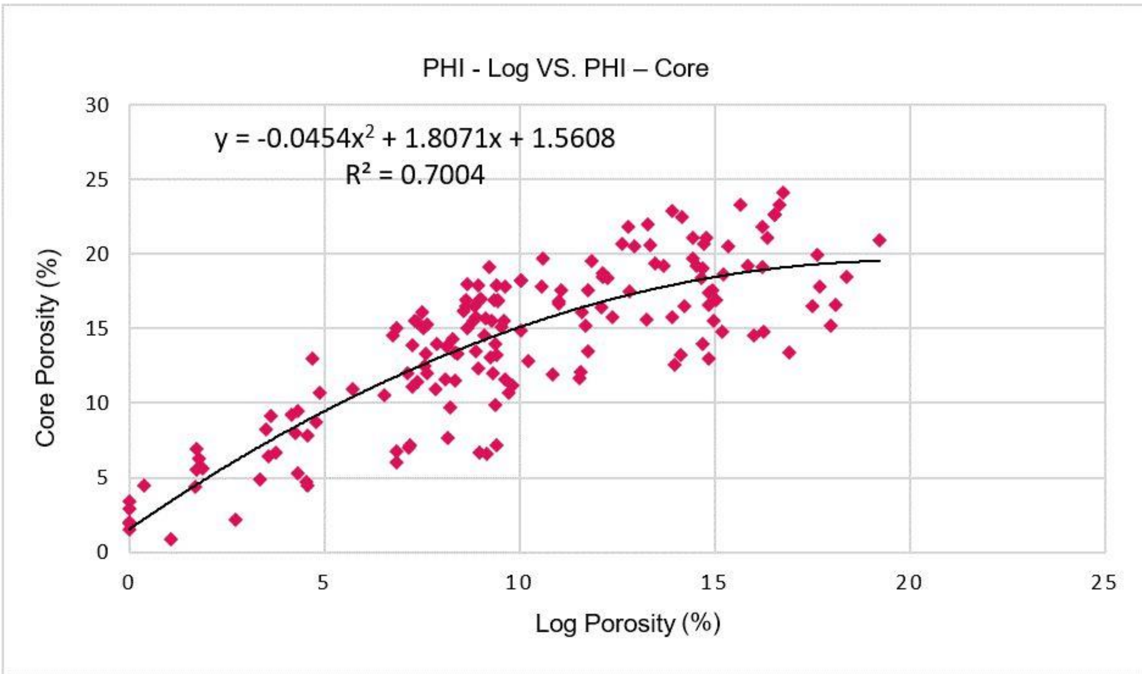

Fig. 6: The correlation between core-derived porosity and log-derived porosity of B-11 well.

The final measurements of effective porosity and secondary porosity index (SPI) of the Mishrif Formation in the Buzurgan oilfield were estimated from the correlation between well logs and core analysis (Fig. 7 and Fig. 8). The final matrix porosity (primary porosity) was obtained from the contrast between final effective porosity and final secondary porosity index (SPI) (Fig. 9). The results showed the effective porosity (PHIE) of the Mishrif Formation ranges from 4% to 18%, (Fig. 7) and (Table 2). The Mb21 unit is characterized by high values of effective porosity (about 18%) compared with the other units. This may refer that this unit represents the rudist-rich facies characterized by high porosity and permeability due to the dissolution process as mentioned by Mahdi et al. (2013) and Jun et al. (2016). The other units that characterize by high effective porosity are MC1 (about 12%) and MC2 (about 16%).

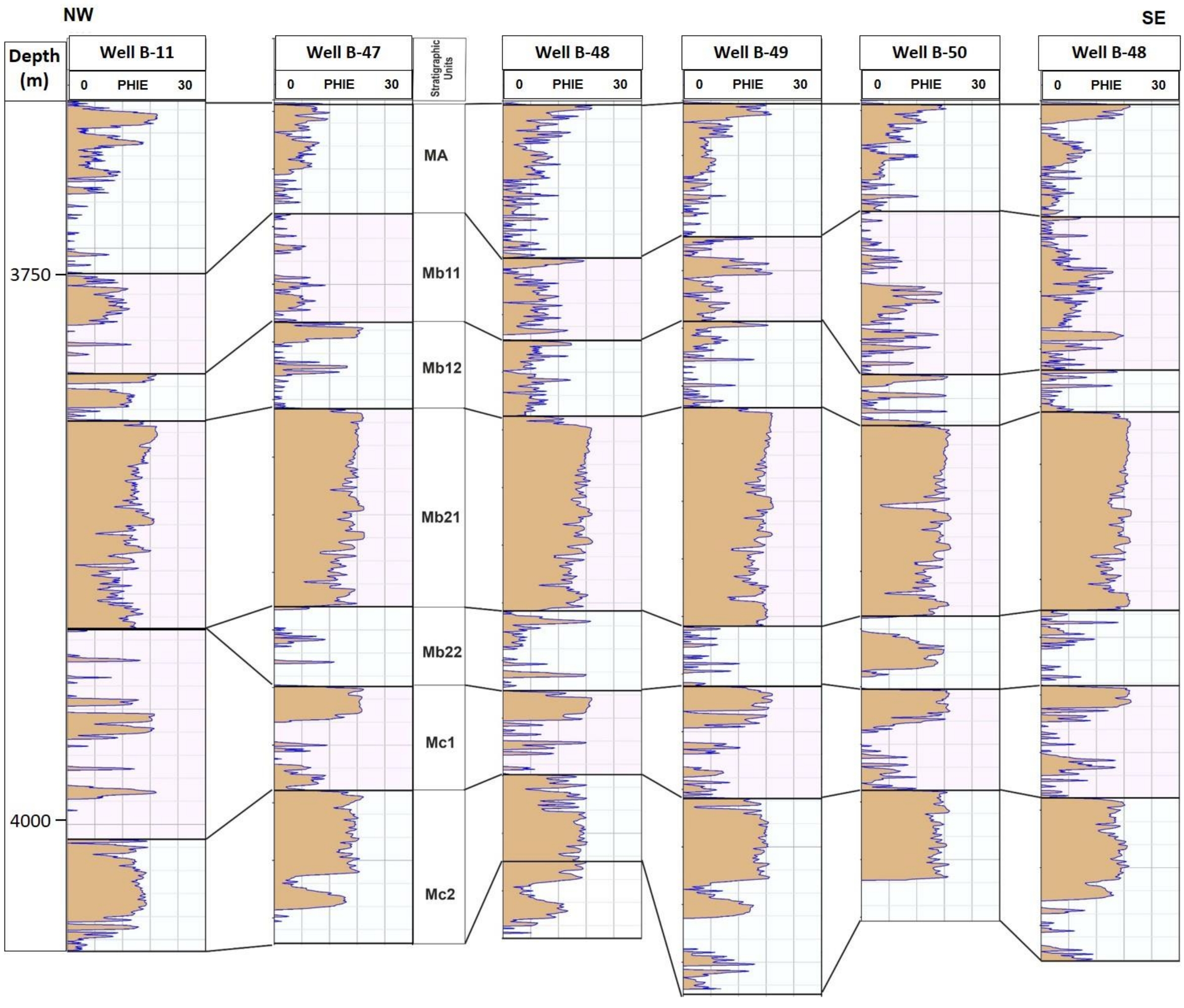

Fig. 7: NW-SE cross-section of effective porosity (PHIE) of the stratigraphic units of the Mishrif Formation for the studied wells.

The average values of secondary porosity (PHIS) of the Mishrif Formation range from 3% to 10%, and the results showed that the Mb21 unit is dominated by high secondary porosity compared with the other stratigraphic units of the Mishrif Formation (Fig. 8) and (Table 2). Unfortunately, this study does not involve a petrographic study to define the type of the secondary porosity, but the previous studies referred that the dissolution is the main type of secondary porosity in the Mishrif Formation, especially in the Mb21 unit that is characterized by rudist facies (example: Mahdi, *et al.*, 2013;

Jun, *et al.*, 2016). Concerning the primary porosity (PHIP), the Mishrif Formation is characterized by low to moderate values (3% to 10%), and the maximum value is noticed in the Mb21 unit (Fig. 9) and (Table 2).

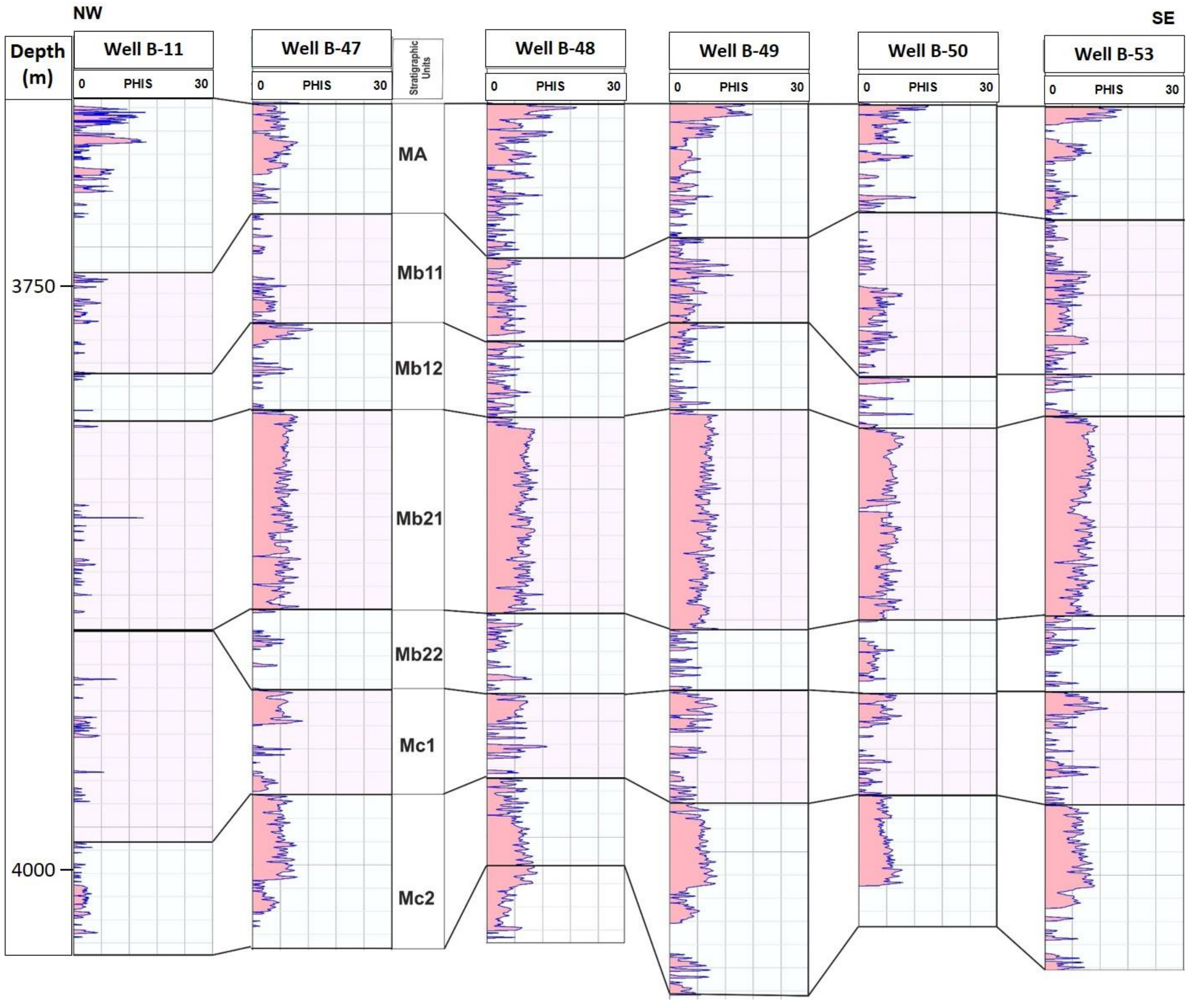

Fig. 6: NW-SE cross-section of secondary porosity (PHIS) of the stratigraphic units of the Mishrif Formation for the studied wells.

4. Water saturation

Water saturation is considered one of the most significant petrophysical parameters in reservoir characterization. Several methods are used to estimate the water saturation, and these methods are; petrophysical models, the saturation-height function from capillary pressure data, and determining the value directly from the core (Al-Bulushi, *et al.*, 2009). An accurate determination of water saturation is required to estimate the hydrocarbon saturation by using the following equation:

$$S_h = 1 - S_w \quad (9)$$

Where: S_h: hydrocarbon saturation, S_w: water saturation

In this study, the water saturation of the Mishrif Formation was calculated by using Archie's equation. The results showed that the Mishrif Formation is characterized by water saturation values ranging between (20% - 90%) (Fig. 10) and (Table 2). The best and largest hydrocarbon accumulations are found in the MB21 unit, followed by MC1 and MC2 units (Fig. 10). It is not clear whether these accumulations of hydrocarbons are moveable or not due to this study does not focus on the mobility of hydrocarbons.

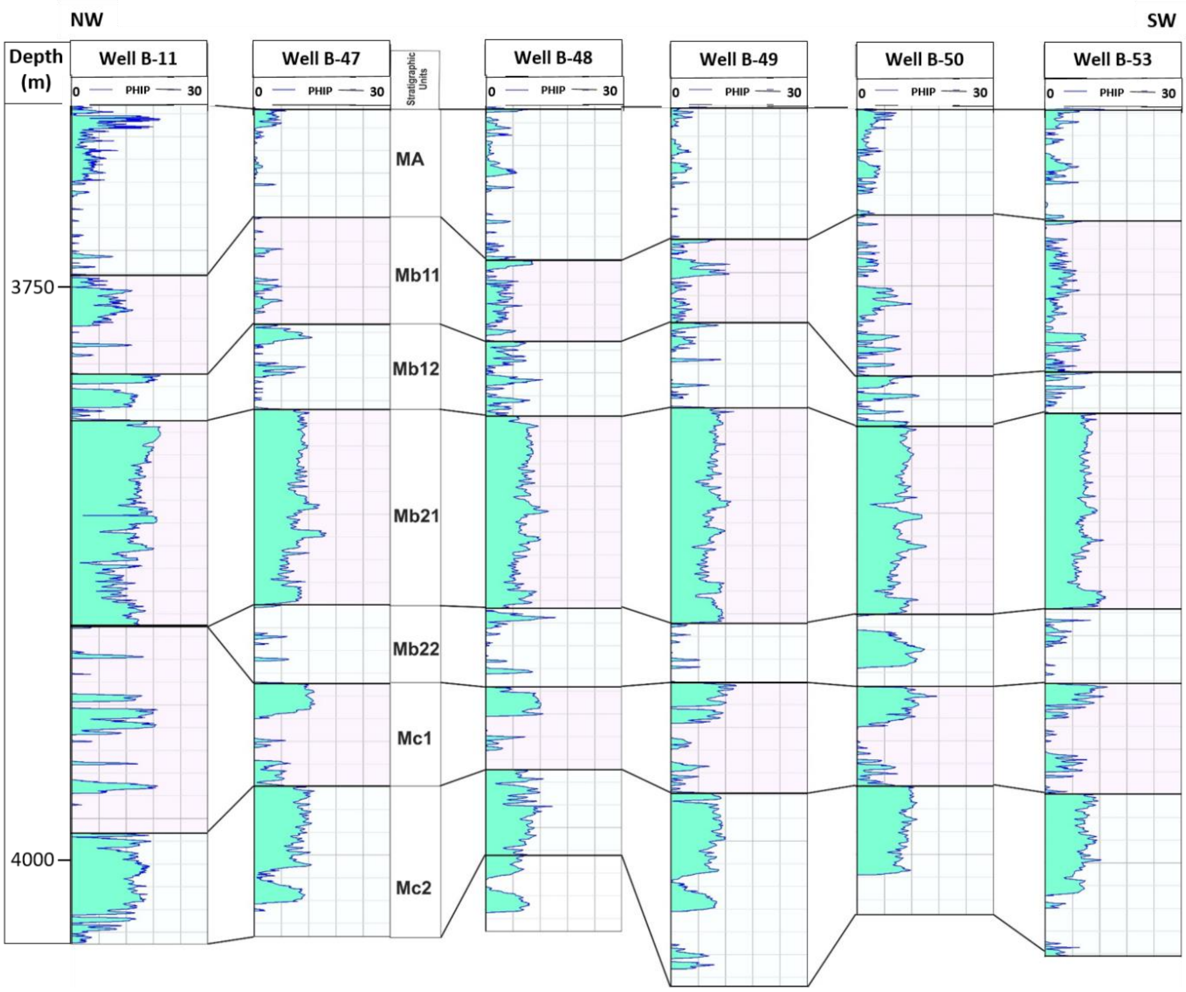

Fig. 9: NW-SE cross-section of primary porosity (PHIP) of the stratigraphic units of the Mishrif Formation for the studied wells.

Table 2: The table shows the average values of effective porosity (PHIE), secondary porosity (PHIS), primary porosity (PHIP), water saturation (Sw), and oil saturation (So) of the stratigraphic units of the Mishrif Formation.

Stratigraphic units	**PHIE (%)**	**PHIS (%)**	**PHIP (%)**	**S_w (%)**	**S_o (%)**
MA	9	5	3	80	20
Mb11	6	3	4	90	10
Mb12	6	3	5	85	15
Mb21	18	10	10	30	70
Mb22	4	3	4	95	5
Mc1	10	4	6	80	20
Mc2	15	6	10	80	20

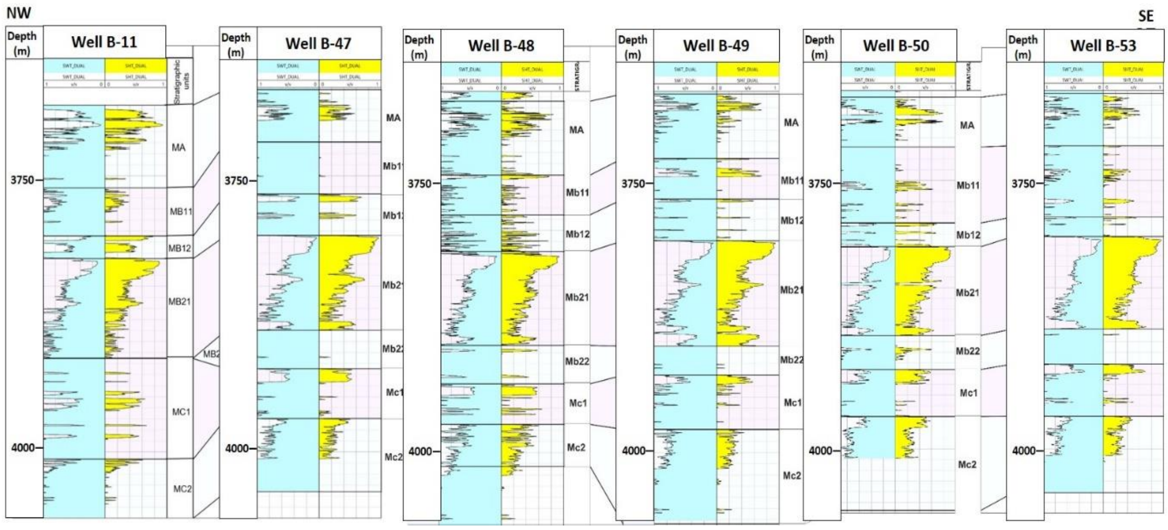

Fig. 10: NW-SE cross-section of water saturation (light blue) and oil saturation (yellow) of the studied wells.

CONCLUSIONS

The lithology of the Mishrif Formation was determined as limestone based on the interpretation of density, neutron, and sonic logs by using an M-N cross plot. The shale volume in the formation varies laterally and vertically, but in general, it is about 20% of the bulk volume. The porosity values of the Mishrif Formation were derived based on the integration between well logs and core analysis. The comparison between the two sets of data showed a good match. The results showed that the Mishrif Formation is dominated by low to medium total porosity values. The MB21 unit of the Mishrif Formation represents the best reservoir in terms of petrophysical properties, where this unit is distinguished by high effective porosity compared with the other units. Concerning the hydrocarbon saturation, the MB21 unit has the largest hydrocarbon accumulations, and this confirms that the MB21 unit represents the main reservoir in the Mishrif Formation.

ACKNOWLEDGMENTS

The authors are grateful to the University of Mosul, College of Petroleum and Mining Engineering for providing access to their facilities, which greatly helped to improve the quality of this research. Besides, the authors would like to acknowledge the Misan Oil Company for providing the well data for this study.

REFERENCES

Al-Ameri, T.K., Al-Marsoumi, S.W. and Al-Musawi, F.A., 2015. Crude oil characterization, molecular affinity, and migration pathways of Halfaya oil field in Mesan Governorate, South Iraq. Arabian Journal of Geosciences, Vol. 8, 7041-7058.

Al-Ameri, Thamer K., Al-Khafaji, Amer J. and Zumberge, J., 2009. Petroleum system analysis of the Mishrif reservoir in the Ratawi, Zubair, North and South Rumaila oil fields, southern Iraq. Geo Arabia, Petrolink, Bahrain 14 (4), 91-108.

Al-Ali, M.M., Mahdi, M.M. and Alali, R.A., 2019. Microfacies and depositional environment of Mishrif Formation, North Rumaila oil field, southern Iraq. Iraqi Geological Journal, Vol. 52, No. 2, 91-104.

Al-Bulushi, N., King, P.R., Blunt, M.J. and Kraaijveld, M., 2009. Development of artificial neural network models for predicting water saturation and fluid distribution. Journal of Petroleum Science and Engineering, Vol. 68, 197-208.

Aldarraji, M.Q. and Almayahi, A.Z., 2019. Seismic structure of Buzurgan oil field, southern Iraq. Iraqi Journal of Science, Vol. 60, No. 3, 610-623.

Alkersan, H., 1975. Depositional environments and geological history of the Mishrif Formation in southern Iraq. 9th Arab Petroleum Congress, Dubai, UAE, paper 121 (section B-3), 1-18.\

Al-Khafaji, A.J., 2015. The Mishrif, Yamama, and Nahr Umr reservoirs petroleum system analysis, Nasiriya oilfield, Southern Iraq. Arabian Journal of Geosciences, Vol. 8, 781-798.

Al-Sakini, J., 1992. Summary of the petroleum geology of Iraq and the Middle East. Northern Oil Company Press, Kirkuk, 179 pp. (in Arabic).

Aqrawi, A.A.M., Thehni, G.A., Sherwani, G.H. and Kareem, B. M. A., 1998. Mid-Cretaceous rudist-bearing carbonates of the Mishrif Formation: An important reservoir sequence in the Mesopotamian Basin, Iraq. Journal of Petroleum Geology, v. 21, No. 1, 57-82.

Bassiouni, Z., 1994. Theory, Measurement, and Interpretation of Well logs. SPE Textbook Series, Vol. 4.

Buday, T., 1980. The Regional Geology of Iraq, Stratigraphy, and Paleogeography. Dar Al Kutub Published house, Mosul, Iraq, 445 pp.

Jassim, S.Z. and Goff, J.C., 2006. Geology of Iraq. Dolin, Prague and Moravian Museum, Brno, Czech Republic, 341 pp.

Jun, W., Rui, G., Limin, Z., Wenke, L., Wen, Z., and Tianxiang, D., 2016. Geological features of grain bank reservoirs and the main controlling factors: A case study on Mishrif Formation, Halfaya Oilfield, Iraq. Petroleum Exploration and Development, Vol. 43, Issue 3, 404-415.

Larionov, V.V., 1969. Borehole Radiometry. Moscow, U.S.S.R, Nedra, 127 pp.

Mahdi, T. A., Aqrawi, A.A.M., Horbury, A.D. and Sherwani, G.H., 2013. Sedimentological characterization of the mid-Cretaceous Mishrif reservoir in southern Mesopotamian Basin, Iraq. Geo Arabia, Vol. 18, No. 1, 139-174.

Owen, R.M.S. and Nasr, S.N., 1958. Stratigraphy of the Kuwait Basrah area. In: Weeks, L.G. (Ed), Habitat of oil. AAPG, Tusla, 1252-1278.

Pickett, G. R., 1973. Pattern Recognition as a Means of Formation Evaluations. The Log Analyst, Vol. 14, No. 4, 3-11.

Reulet, J., 1970. Sedimentological study of the Mishrif Reservoir. Department of Exploration, ELF – Iraq.

Sang, H., Lin, C. and Jiang, Y., 2017. Sequence stratigraphy and sedimentary study on Mishrif formation of Fauqi Oilfield of Missan in southeast Iraq. IOP Conf. Series: Earth and Environmental Science, 64.

Schlumberger, 2011. Well log interpretation chartbook.

Schlumberger, 1989. Log interpretation principles/applications. Schlumberger Wireline and Testing, 241 pp.

Schlumberger, 1974. Log interpretation manual/applications. Schlumberger well service, V. 2, 116 pp.

Schlumberger, 1972. Log Interpretation – Principle. New York, Schlumberger, Vol. 2, 116 pp.

Schon, J. H., 2011. Physical properties of rocks. Vol. 8, Elsevier, Amsterdam, The Netherlands.

Sherwani, G.H. and Mohammed, I.Q., 1993. Sedimentological factors controlling the depositional environment of Cenomanian Mishrif Formation, southern Iraq. Iraqi Geological Journal, Vol. 26, 122-134.

Tiab, D. and Donaldson, E. C., 2012. Petrophysics, Theory, and Practice of Measuring Reservoir Rock and Fluid Transport Properties. Third edition, Elsevier, Amsterdam, The Netherlands.